Supporting Information (SI) Appendix

SI Methods

Construction of GPAT4, GPAT5 and GPAT6 Yeast Expression Vectors. GPAT5 cDNA was obtained from Incyte, GPAT4 and GPAT6 cDNA were obtained from Arabidopsis Biological Resource Center. *GPAT5* was cloned into Topo GATEWAY entry vector pENTR/D TOPO using forward primer 5'-CACCAAGAAATGGTTATGGAGCAAGCTG-3' and reverse primer 5'-CAATGGAGACAAGGCTCGAAAG-3'. Then it was introduced into the Gateway destination vector pYES-DEST52 through LR recombination reaction by following the manufacturer's instruction (Invitrogen). The coding sequence of *GPAT4* was amplified by PCR using forward primer 5'-CACACGGTACCATGTCTCCGGCGAAGA-3' (*Kpn*I) and reverse primer 5'-CACACTCTAGATTACTCCATGGACTTGGT-3' (*Xba*I). The PCR product was first cloned into pGEM-T easy vector, then ligated into yeast expression vector pYES2/CT as a *Kpn*I-*Xba*I fragment. The *GPAT6* coding sequence was amplified by PCR using forward primer 5'- CGC GGA TCC AAA ATG GGA GCT CAG GAG AAA-3' (*BamH* I), and reverse primer 5'-CCG GAA TTC TCA CGT CTT CTC CTT CTT C-3' (*EcoR* I). The PCR product was restricted with *BamH*I and *EcoR*I and ligated to the vector pYES2/CT which has been restricted by the same enzymes. The integrity of the constructs, GPAT5/pYES-DEST52, GPAT4/pYES2-CT and GPAT6/pYES2-CT were verified by sequencing.

Construction of GPAT5 and GPAT6 Plasmids for Wheat Germ Expression. The coding sequence of GPAT6 was amplified by PCR as *BamH* I-*EcoR* I fragment as mentioned above. The PCR product was first cloned into pGEM-T easy vector, then cut with *Nco* I / *Pst* I, and the resulting DNA fragment was directly inserted into RTS pIVEX wheat germ His_6-tag vector pIVEX 1.4 WG. *Nco* I and *Xma* I restriction sites were added to the coding sequence of GPAT5 by PCR with forward primer 5'-CATGCCATGGTTATGGAGCAAGCT-3' (*Nco* I) and reverse primer 5'-TCACCCCGGGTCAATGGAGACAAGGCTCGA-3' (*Xma* I). The *Nco* I-*Xma* I fragment was directly inserted into RTS pIVEX wheat germ His_6-tag vector pIVEX 1.4 WG. The integrity of the constructs, GPAT5/pIVEX 1.4 WG and GPAT6/pIVEX 1.4 WG was verified by sequencing.

Synthesis and Identification of ω-oxidized Acyl-CoAs. 16-Hydroxyhexadecanoic acid (98%), hexadecane-1,16-dioic acid (>98%) and docosane-1,22-dioic acid (85%, purified to >95% before use) were purchased from Sigma-Aldrich. 22-Hydroxydocosanoic acid (>98%) was from Matreya**,** LLC. Octadec-9*cis*-ene-1,18-dioic acid was a gift from Cognis corporation (Ohio). 18-Hydroxyoctadec-9*cis*-enoic acid was purified from tobacco stigma lipids (1) by transmethylation, preparative-TLC (K6 plate, hexane:diethyl ether, 65:35, R_f = 0.3), C18 reversed-phase HPLC (semi-preparative column 218TP510, 10 mm × 250 mm, isocratic elution with 55% acetonitrile/water), and finally saponification of the purified fatty acid methyl ester. Omega-oxidized acyl-CoAs were synthesized from the corresponding fatty acids using carbonyldiimidazole (CDI) method (2) and precipitated with 7% perchloric acid. After extraction of unreacted free fatty acid

with hexane, the acyl-CoA precipitates were washed with 0.7% perchloric acid, re-dissolved in 0.01 M NaOAc/EtOH (1:1, pH 5.2) and stored at -20 °C before use. The purity of the acyl-CoA was checked by analytical TLC (silica gel K6, butanol:water:acetic acid (5:3:2) (3), and the concentration of synthesized acyl-CoAs was determined by UV spectroscopy using an extinction coefficient of 16400 at 260 nm (4).

To identify the ω-oxidized acyl-CoAs, the acyl-CoA stock solutions were further diluted with methanol:0.2% aqueous triethylamine (4:1) to 10 μM for analysis by electrospray ionization mass spectrometry (ESI-MS) in positive ion mode with sodium adduct (5, 6). 10 μl of sample was introduced to the electrospray source by flow injection into a methanol:0.2% aq. triethylamine (4:1) solution at a flow rate of 0.1 ml/min. The capillary, cone and extractor voltages were 3.2 kV, 45 V and 2.0 V, respectively. The source and desolvation temperatures were 110 °C and 350 °C, respectively. The desolvation gas flow rate was 400 l/hr. The cone gas flow rate was 20 l/hr. Mass spectra were collected for 2 min; the *m*/*z* range scanned in the MS measurements was from 400 to 2000 (1 sec/scan) and in the MS/MS mode from 200 to the mass of the parent ion. Argon was used as the collision gas at a pressure of 2×10^{-3} mbar. The optimized collision energy was set at 29V. The optimized cone voltage was 55V. Mass spectra data were acquired with MassLynx 4.0 software. Each product was identified by its characteristic acyl pantetheine group, the fragment remaining after neutral loss of 507, and its related $[M+1]^+$ peak. (***Table S1***). Ions corresponding to the bis-CoA thioester adduct of DCAs were not observed.

Synthesis and Identification of DCA *sn*-1 and *sn*-2 MAGs. DCA-MAGs were synthesized by modification of other protocols (7-10). In brief, to synthesize DCA *sn*-2 MAG, 4-(Dimethylamino)pyridine (9 μmole) and *N*-(3-dimethylaminopropyl)-*N*′-ethylcarbodiimide hydrochloride (18 μmole) were added to a solution of 1,3-benzylidene glycerol (27 μmole) and DCA free acid (18 μmole) in anhydrous dichloromethane or tetrahydrofuran, and the resulting solution was stirred at room temperature over night. After 24 hours, the reaction mixture was diluted with ethyl acetate, and washed with water and saturated NaCl solution. The organic layer was dried under N_2. To remove the benzylidene group, trimethyl borate was added to dissolve the above solvent extract. After adding boric acid, the reaction mixture was stirred at 98 °C for 20 min, dried under N_2, heated for another 10 min, cooled to room temperature and washed with diethyl ether/water. The organic phase was applied to borate-TLC and developed with chloroform:acetone (1:1). The DCA *sn*-2 MAG was eluted from the borate-silica with chloroform:acetone (1:1). The solvent eluent was washed with ice cold water, and the organic phase was dried down under N_2, stored at -20 °C before use. To synthesize DCA *sn*-1 MAG, (*R*) (−)-2,2-dimethyl-1,3-dioxolane-4-methanol (27 μmole) replaced 1,3-benzylidene glycerol. The purified DCA *sn*-1 and *sn*-2 MAGs were trimethylsilylated with pyridine/BSTFA (1:1, v/v) at 110°C for 10 min and analyzed by GC-MS using a 30 m DB-5 capillary column, temperature programmed from 130 °C to 330 °C, in line with a MSD 5972 mass analyzer (70 eV, scanning 40 to 700 atomic mass units)

The mass spectra of the tris-trimethylsilyl (TMSi) derivatives of the synthetic DCA-MAGs are shown in ***Fig. S3***. These spectra can be compared with the bis-trimethylsilyl (TMSi) mass spectra of MAGs of simple fatty acids such as palmitate (11) or tetracosanoate (12). The addition of an ω-TMSi ester group does not change the basic

fragmentation pattern for either α- or β-MAGs. The α-MAG spectra are still dominated by strong $(M\text{-}103)^+$ ions, that is $(M\text{-}CH_2OTMSi)^+$ ions derived from a cleavage between the TMSi-ether groups (m/z = 473 in Fig S3(A) and m/z = 499 in Fig S3(C)). The β-MAGs show a distinctive m/z = 218 fragment resulting from the loss of the ω-TMSi fatty acid $(M - RCOOH)^+$. Acylium (RCO^+) and $(RCO + 74)^+$ fragments, at m/z = 341 and 415 respectively for C16:0 DCA-MAG and at m/z = 367 and 441 for C18:1 DCA-MAG, are seen in the spectra of both isomers. The $(RCO + 74)^+$ fragmentation is due to the loss of $Me_3SiOSiMe_2CH_2$. In addition to distinctive mass spectra, α- or β-MAG isomers can be readily distinguished by their GC retention times, with β-MAGs eluting ahead of α-MAGs.

1. Matsuzaki T, Koiwai A, Kawashima N (1983) Changes in stigma-specific lipids of tobacco plant during flower development. *Plant Cell Physiol* 24:207-213.
2. Kawaguchi A, Yoshimura T, Okuda S (1981) A new method for the preparation of acyl-CoA thioesters. *J Biochem* 89:337-339.
3. Loncaric C, Merriweather E, Walker KD (2006) Profiling a taxol pathway 10β-acetyltransferase: Assessment of the specificity and the production of baccatin III by *in vivo* acetylation in *E. Coli*. *Chem Biol* 13:309-317.
4. Panuganti SD, Penn JM, Moore KH (2003) Hepatic enzymatic synthesis and hydrolysis of CoA esters of solvent-derived oxa acids. *J Biochem Mol Toxicol* 17:76-85.
5. Sun D, Cree MG, Wolfe RR (2006) Quantification of the concentration and ^{13}C tracer enrichment of long-chain fatty acyl-coenzyme A in muscle by liquid chromatography/mass spectrometry. *Anal Biochem* 349:87-95.
6. Magnes C, Sinner FM, Regittnig W, Pieber TR (2005) LC/MS/MS method for quantitative determination of long-chain fatty acyl-CoAs. *Anal Chem* 77:2889-2894.
7. Martin JB (1953) Preparation of saturated and unsaturated symmetrical monoglycerides. *J Am Chem Soc* 75:5482-5483.
8. Haraldsson GG, Halldorsson A, Kulas E (2000) Chemoenzymatic synthesis of structured triacylglycerols containing eicosapentaenoic and docosahexaenoic acids. *J Am Oil Chem Soc* 77:1139-1145.
9. Suhara Y, et al. (2007) Synthesis and biological evaluation of several structural analogs of 2-arachidonoylglycerol, an endogenous cannabinoid receptor ligand. *Bioorg Med Chem* 15:854-867.
10. Sugiura T, et al. (1999) Evidence that the cannabinoid CB1 receptor is a 2-arachidonoylglycerol receptor - structure-activity relationship of 2-arachidonoylglycerol ether-linked analogues, and related compounds. *J Biol Chem* 274:2794-2801.
11. Murphy RC (1993) in *Mass Spectroscopy of Lipids—Handbook of Lipid Research*. (Springer, New York), pp 206.
12. Li Y, Beisson F, Ohlrogge J, Pollard M (2007) Monoacylglycerols are components of root waxes and can be produced in the aerial cuticle by ectopic expression of a suberin-associated acyltransferase. *Plant Physiol* 144:1267-1277.
13. von Heijne G (1992) Membrane protein structure prediction, hydrophobicity analysis and the positive-inside rule. *J Mol Biol*, 225: 487-494.

14. Engelman DM , Steitz TA, Goldman A (1986) Identifying nonpolar transbilayer helices in amino acid sequences of membrane proteins *Annu Rev Biophys Chem* 15: 321-353.

Table Legend

Table S1. Identification of omega-hydroxy (ω-OH)- and Dicarboxylic Acid (DCA)-CoAs by ESI-MS/MS. (***A***) Characteristic fragmentation of protonated acyl-CoA by neutral loss of 507 to give the protonated acyl pantetheine group. Specific *m/z* values observed for $[M + H]^+$ and [acyl pantetheine + H^+] are tabulated below. (***B***) ESI-MS/MS spectra of DCA-CoAs.

Figure Legends

Fig. S1. Radio-TLC Images of Product Distribution of GPAT Assay in Either (A) Yeast *gat1*Δ Strain or (B) Wheat Germ Cell-free Translation System. After assay, the quenched reaction mixture was directly applied to TLC plate (K6), and developed with solvent system: chloroform:methanol:acetic acid:water (85:15:10:3.5). LPA and MAG were tentatively identified by comparison with 18:1 *sn*-1 LPA and 18:1 MAG standards, respectively. The large spot at the origin is unreacted [^{14}C]G3P.

Fig. S2. Time Course of C16:0 DCA-MAG Formation from GPAT6 in Yeast *gat1*Δ Strain. Assays contained 10 μg of microsomal protein from yeast expressing *GPAT6*. After assay, the reaction mixture was directly applied to K6 TLC plate for analysis as described in Fig. S1. ^{14}C-Labeled MAG (nmol) formation was linear with assay time.

Fig. S3. Electron Impact Mass Spectra (EI-MS) of tris-Trimethylsilyl (TMS) Derivatives of Synthetic (*A*) C16:0 DCA *sn*-1 MAG, (*B*) C16:0 DCA *sn*-2 MAG, (*C*) C18:1 DCA *sn*-1 MAG and (*D*) C18:1 DCA *sn*-2 MAG. The molecular weights for C16:0 DCA-MAG and C18:1 DCA-MAG are 576 and 602, respectively; $(M-15)^+$ peaks are observed at 561 and 587 respectively. A further description of the diagnostic mass fragmentation of the MAG isomers is given in the section "Synthesis and Identification of DCA *sn*-1 and *sn*-2 MAGs."

Fig. S4. Identification of 18:1 DCA *sn*-2 MAG from GPAT4 assay by GC-MS. (***A***) GC chromatogram of TLC fraction containing 18:1 DCA *sn*-2 MAG (***B***) EI-MS spectrum of 18:1 DCA *sn*-2 MAG-tris-trimethylsilyl derivative (peak at 34.49 min). See Fig.S3 for spectrum of standard.

Fig. S5. GPAT4 Activity Assay Results under Various Assay Conditions. (***A***) [^{14}C]G3P+18:1 DCA-CoA (***B***)18:1 DCA-CoA alone and (***C***) [^{14}C]G3P alone. (***D***) GPAT assay with yeast empty vector transformant using [^{14}C]G3P and 18:1 DCA-CoA. No MAG products were observed under the conditions of ***(B)-(D)***. The 18:1 DCA *sn*-1 MAG product partly overlaps with an unknown peak at 34.91 minutes, but can be resolved by single ion monitoring. It represents about 20% of the mass of the 2-isomer at 34.49 minutes in panel (***A***).

Fig. S6. **Radio-TLC of Positional Analysis of C16:0 DCA-LPA From GPAT5 Assay**. (***A***) Radio-TLC image of GPAT assay of yeast *gat1*Δ strain containing empty vector, GPAT4, GPAT5 or GPAT6. [^{14}C]G3P and C16:0 DCA-CoA were used as substrates.

C16:0 DCA-LPA was the only product for GPAT5. (***B***) Borate-TLC for GPAT5 assay after alkaline phosphatase (AP) treatment. Products C16:0 DCA *sn*-1 and *sn*-2 MAGs were identified by co-migration with C18:1 DCA *sn*-1 and *sn*-2 MAG standards (dotted circles).

Fig. S7. GPAT5 Activity with Very Long Chain Acyl-CoAs. ***A***) GPAT5 assay with saturated C22, C22-ωOH or C22-DCA acyl-CoAs in GPAT5-transformed yeast *(gat1*Δ) microsomes. Assay product (nmol) was LPA. Values are mean ± s.d. (n=3). ***B***) Radio-borate TLC image of positional analysis of C22:0-LPA. (solvent system: chloroform:acetone (1:1). C22:0 *sn*-2 MAG was the major product.

Fig. S8. **Complete Models for N- and C-terminal Domains of GPAT6 Based on *Methanococcus jannaschii* Phosphoserine Phosphatase (PDB: 1F5S) and Squash Glycerol-3-Phosphate (1)-Acyltransferase (PDB: 1K30), respectively.** Cartoon representation is colored by index (N-terminus (blue) to C-terminus (red)). Active site residues in N-terminal domain are shown as in Figure 5.

Fig. S9. Positional Analysis of C16:0 DCA-LPA from Assay of GPAT6 Site-Directed Mutants in Wheat Germ Cell-Free Translation System. GPAT assays were conducted using ^{14}C-G3P and C16:0 DCA-CoA as substrates. Two microliters of wheat germ translation reaction mixture of GPAT6 mutant (D29E, K178L or D200K) were used as the enzyme source, with GPAT6-WT and empty vector as the controls. (***A***) Radio-TLC image of product distribution of GPAT6 assay. C16:0 DCA-LPA was the major product for all three mutants. (***B,C***) Regiochemical analysis of LPA from assays of GPAT6 mutant forms. (***B***) Borate-TLC of products after immediate alkaline phosphatase (AP) treatment of the assay reaction. Products C16:0 DCA *sn*-1 and *sn*-2 MAGs were identified by co-migration with C18:1 DCA *sn*-1 and *sn*-2 MAG standards (dotted circles). (***C***) Product quantitation from borate-TLC analysis. In all three cases, *sn*-2 MAG is the predominant product derived from LPA hydrolysis.

Fig. S10. Hydropathy plot for GPAT4, GPAT5, and GPAT6 sequences from TopPred (13) according to the Goldman-Engelman-Steitz hydrophobicity scale (14). The dotted line indicates an approximate cutoff above which transmembrane segments are likely. A transmembrane or membrane-associated region is predicted for residues 244-264 (GPAT4), 233-270 (GPAT5), and 246-266 (GPAT6). These residues separate the active/inactive phosphatase and acyltransferase domains of the proteins.

Fig. S11. **Sequence Alignment of N-terminal Amino Acids of GPAT4 and GPAT6 with Primitive Moss, *Physcomitrella patens* (XP_n) and Spikemoss, *Selaginella moellendorffii* (jgi_n).** Partial sequences containing conserved motif I and III are shown. The conserved amino acid residues required for PSP activity in motif I and III are highlighted with colors.

Table S1. Identification of omega-hydroxy (ω-OH)- and Dicarboxylic Acid (DCA)-CoAs by ESI-MS/MS. (***A***) Characteristic fragmentation of protonated acyl-CoA by neutral loss of 507 to give the protonated acyl pantetheine group. Specific m/z values observed for $[M + H]^+$ and [acyl pantetheine + H^+] are tabulated below. (***B***) ESI-MS/MS spectra of DCA-CoAs.

A

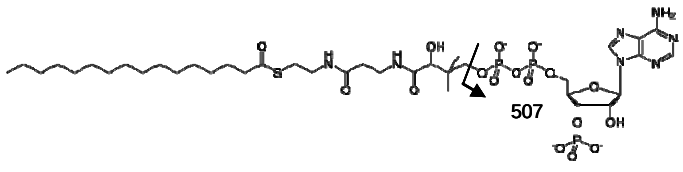

Acyl CoA	$[M+H]^+$	[acyl pantetheine+H]$^+$
16:0 ω-OH	1022.4	515.3
16:0 DCA	1036.3	529.4
18:1 ω-OH	1048.3	541.3
18:1 DCA	1062.4	555.4
22:0 ω-OH	1106.5	599.5
22:0 DCA	1120.3	613.3

B

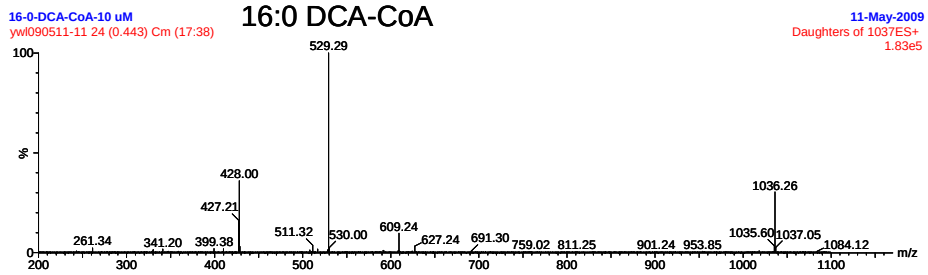

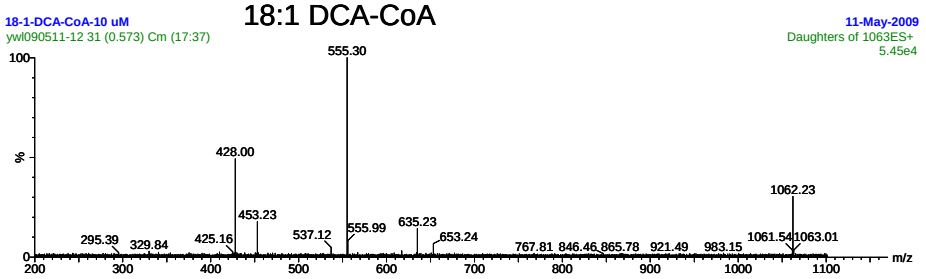

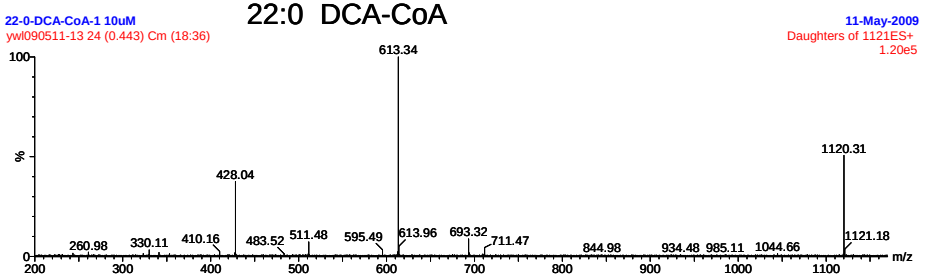

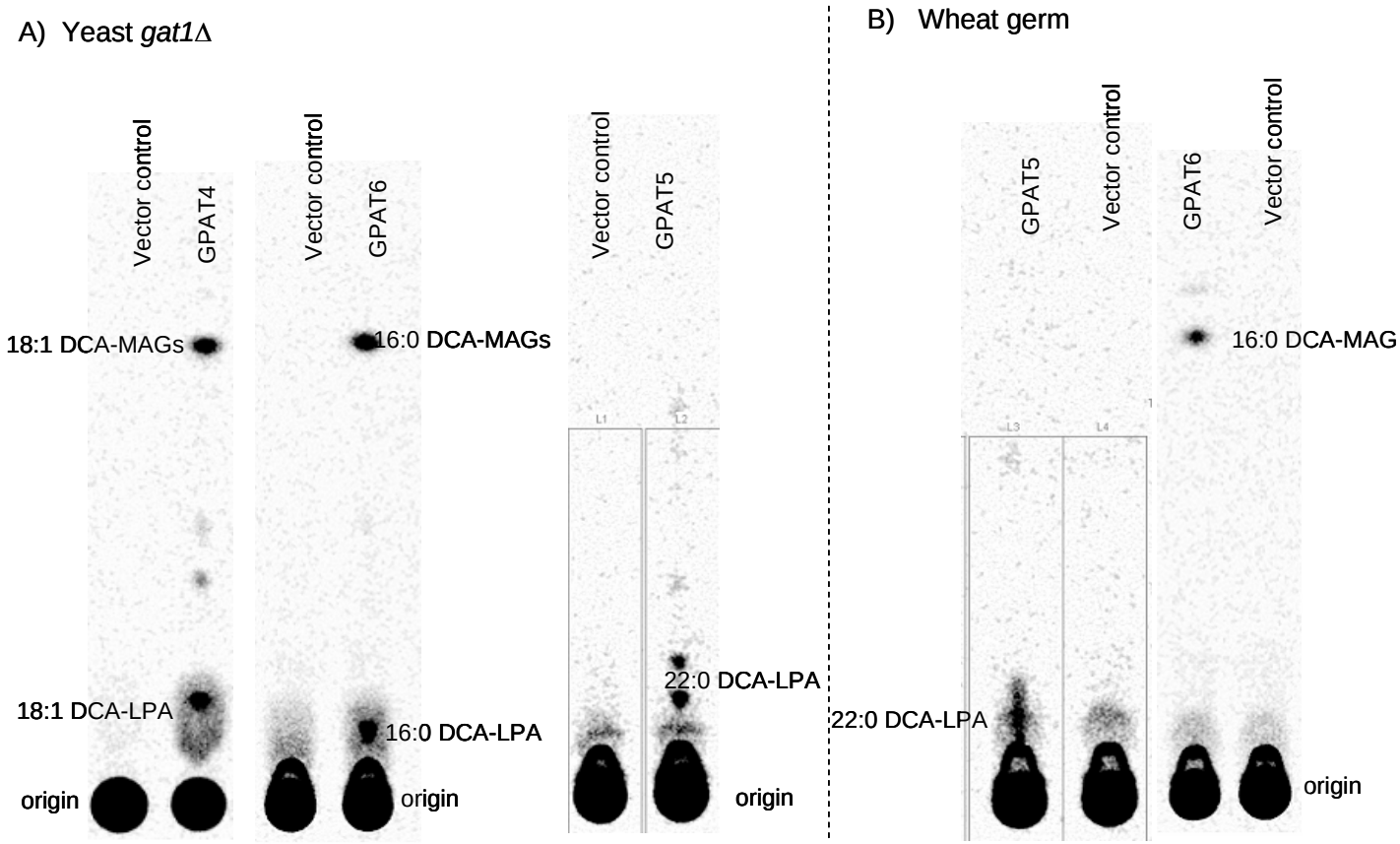

Fig. S1. Radio-TLC Images of Product Distribution of GPAT Assay in Either (A) Yeast *gat1*Δ Strain or (B) Wheat Germ Cell-free Translation System. After assay, the quenched reaction mixture was directly applied to TLC plate (K6), and developed with solvent system: chloroform:methanol:acetic acid:water (85:15:10:3.5). LPA and MAG were tentatively identified by comparison with 18:1 *sn*-1 LPA and 18:1 MAG standards, respectively. The large spot at the origin is unreacted [^{14}C]G3P.

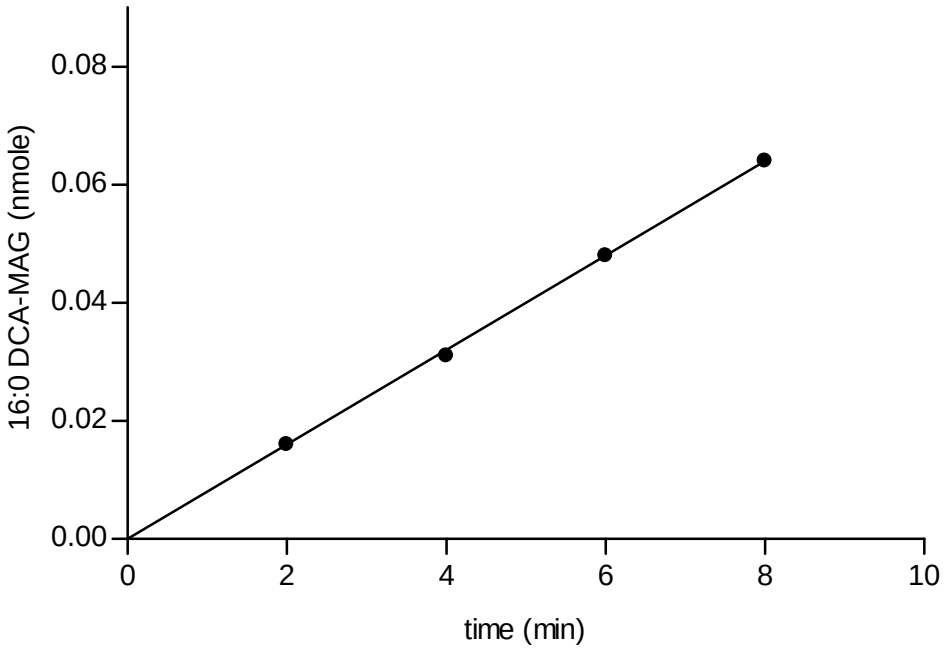

Fig. S2. Time Course of C16:0 DCA-MAG Formation from GPAT6 in Yeast *gat1*Δ Strain. Assays contained 10 μg of microsomal protein from yeast expressing *GPAT6*. After assay, the reaction mixture was directly applied to K6 TLC plate for analysis as described in Fig. S1. ^{14}C-Labeled MAG (nmol) formation was linear with assay time.

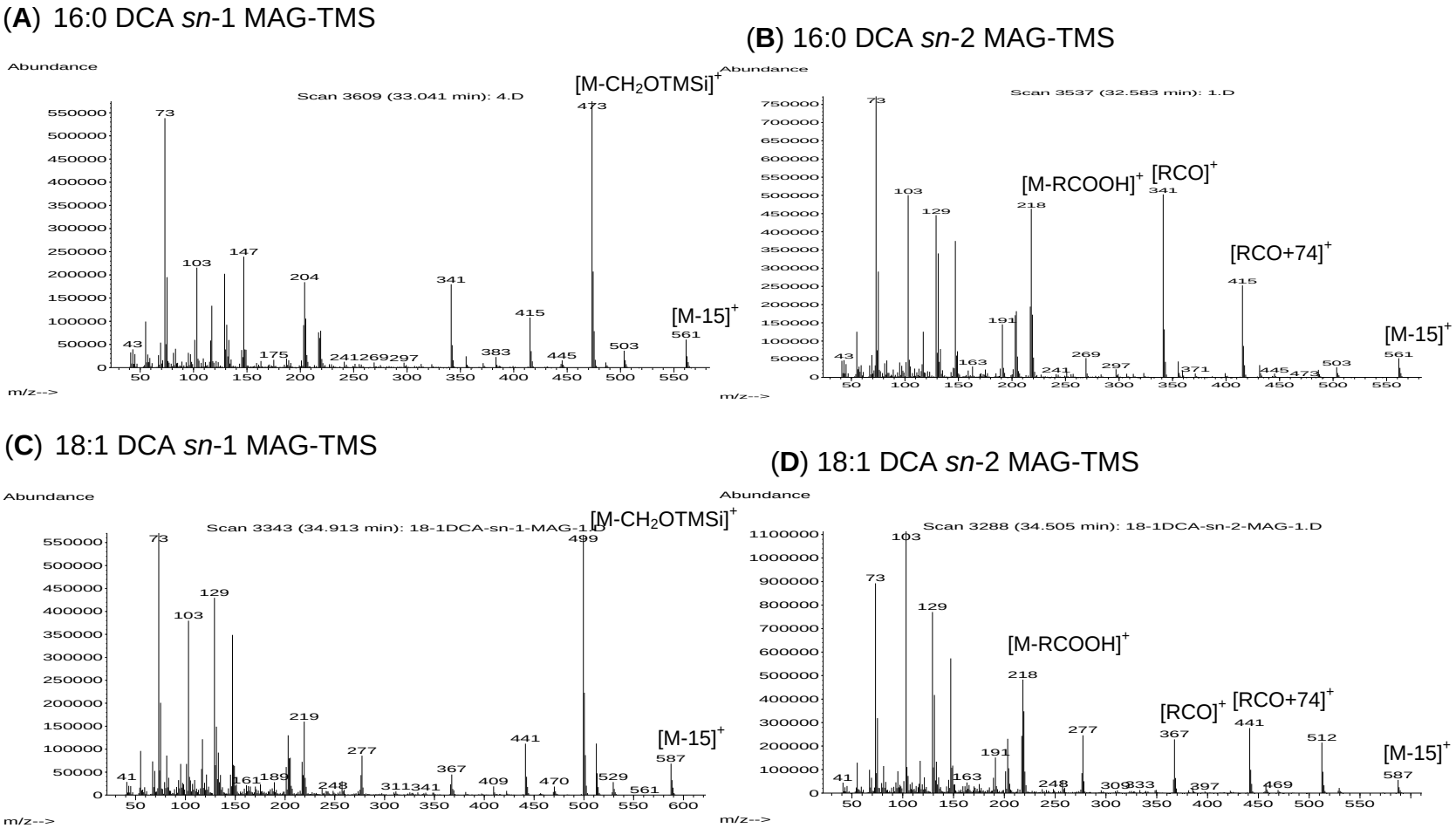

Fig. S3. Electron Impact Mass Spectra (EI-MS) of tris-Trimethylsilyl (TMS) Derivatives of Synthetic (*A*) C16:0 DCA *sn*-1 MAG, (*B*) C16:0 DCA *sn*-2 MAG, (*C*) C18:1 DCA *sn*-1 MAG and (*D*) C18:1 DCA *sn*-2 MAG. The molecular weights for C16:0 DCA-MAG and C18:1 DCA-MAG are 576 and 602, respectively; $(M-15)^+$ peaks are observed at 561 and 587 respectively. A further description of the diagnostic mass fragmentation of the MAG isomers is given in the section "Synthesis and Identification of DCA *sn*-1 and *sn*-2 MAGs."

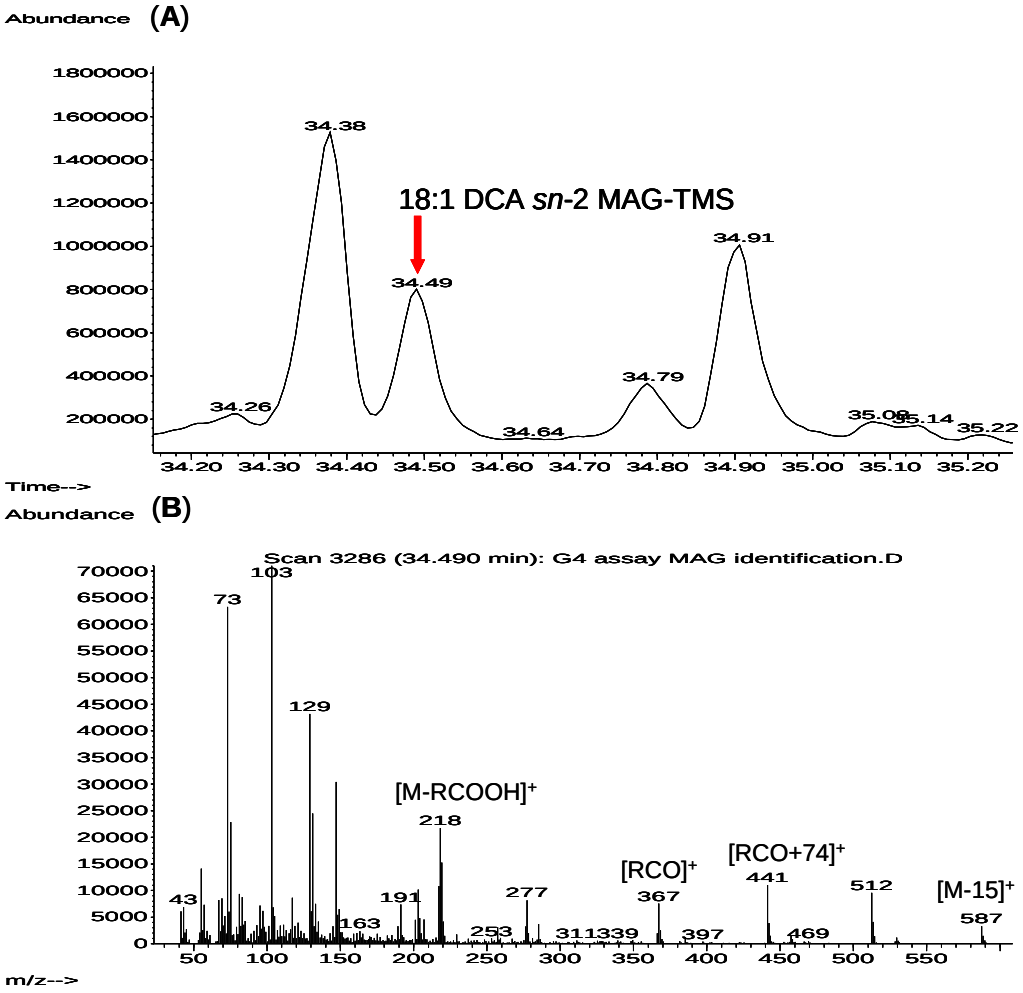

Fig. S4. Identification of 18:1 DCA *sn*-2 MAG from GPAT4 assay by GC-MS. (***A***) GC chromatogram of TLC fraction containing 18:1 DCA *sn*-2 MAG (***B***) EI-MS spectrum of 18:1 DCA *sn*-2 MAG-tris-trimethylsilyl derivative (peak at 34.49 min). See Fig.S3 for spectrum of standard.

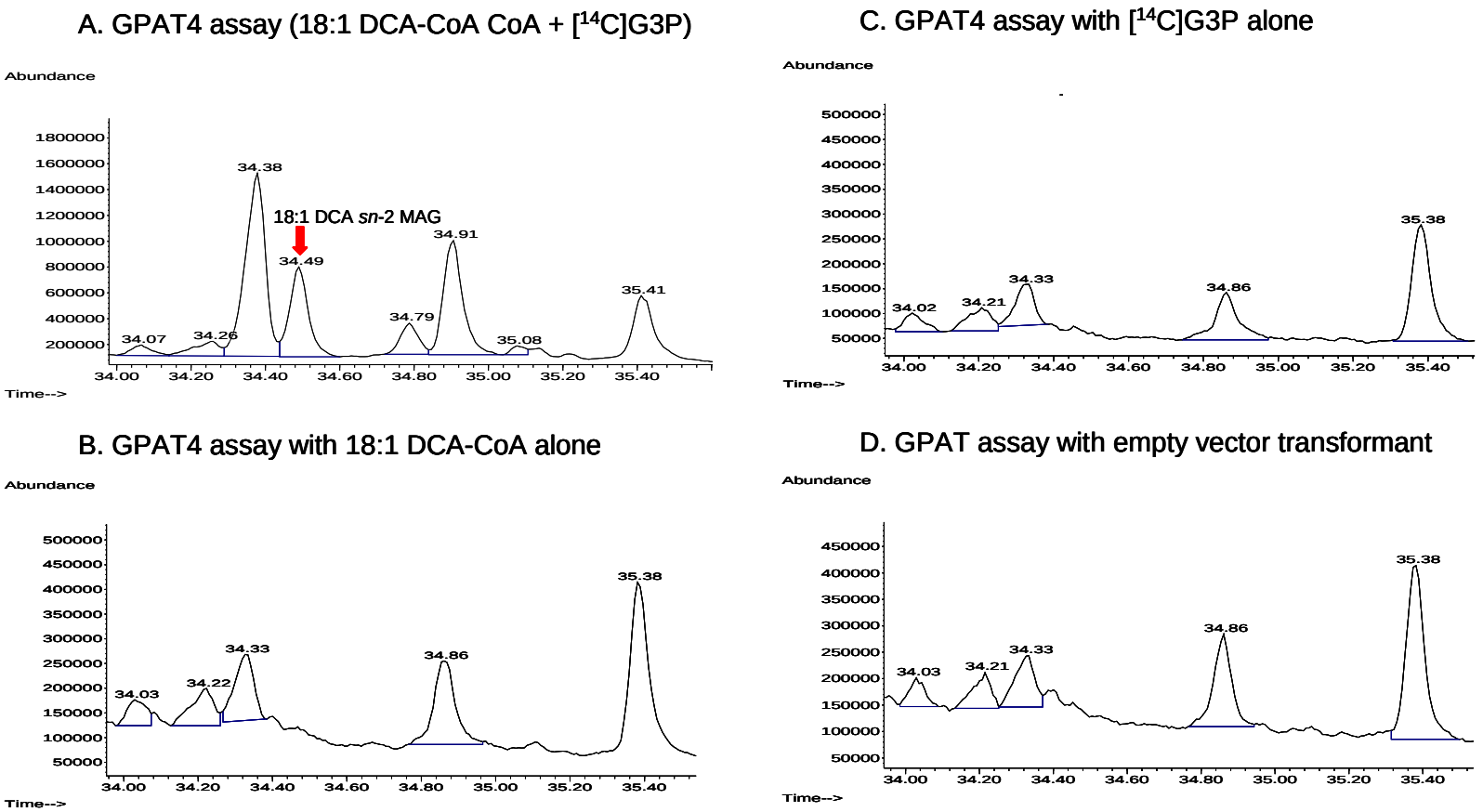

Fig. S5. GPAT4 Activity Assay Results under Various Assay Conditions. (***A***)[^{14}C]G3P+18:1 DCA-CoA (***B***)18:1 DCA-CoA alone and (***C***) [^{14}C]G3P alone. (***D***) GPAT assay with yeast empty vector transformant using [^{14}C]G3P and 18:1 DCA-CoA. No MAG products were observed under the conditions of ***(B)-(D)***. The 18:1 DCA *sn*-1 MAG product partly overlaps with an unknown peak at 34.91 minutes, but can be resolved by single ion monitoring. It represents about 20% of the mass of the 2-isomer at 34.49 minutes in panel (***A***).

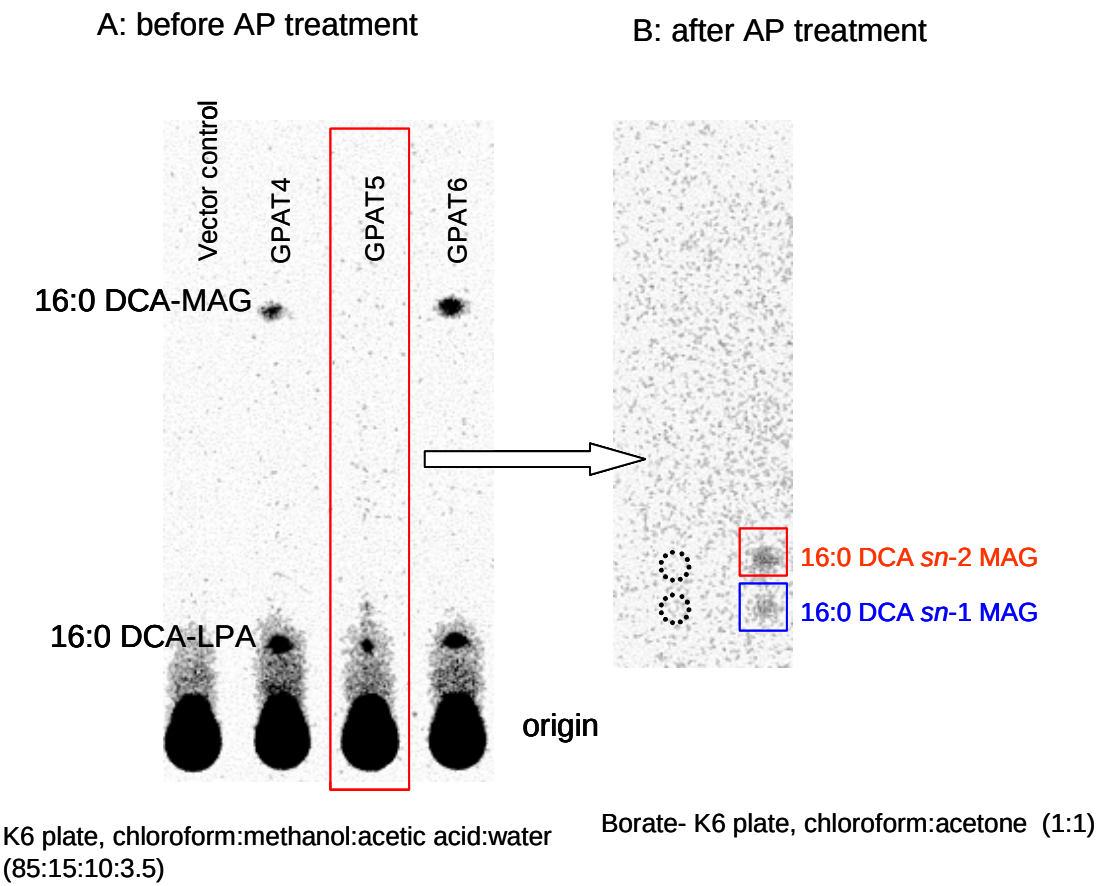

Fig. S6. **Radio-TLC of Positional Analysis of C16:0 DCA-LPA From GPAT5 Assay**. (***A***) Radio-TLC image of GPAT assay of yeast *gat1*Δ strain containing empty vector, GPAT4, GPAT5 or GPAT6. [^{14}C]G3P and C16:0 DCA-CoA were used as substrates. C16:0 DCA-LPA was the only product for GPAT5. (***B***) Borate-TLC for GPAT5 assay after alkaline phosphatase (AP) treatment. Products C16:0 DCA *sn*-1 and *sn*-2 MAGs were identified by comigration with C18:1 DCA *sn*-1 and *sn*-2 MAG standards (dotted circles).

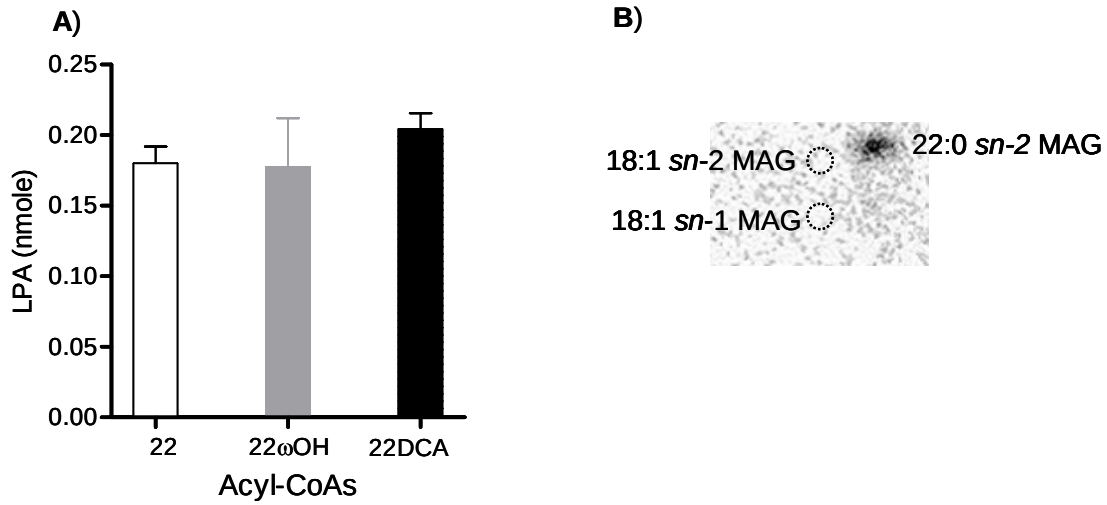

Fig. S7. GPAT5 Activity with Very Long Chain Acyl-CoAs. ***A***) GPAT5 assay with saturated C22 / C22ωOH / C22 DCA-CoAs in GPAT5-transformed yeast *(gat1*Δ) microsomes. Assay product (nmol) was LPA. Values are mean ± s.d. (n=3). ***B***) Radio-borate TLC image of positional analysis of C22:0-LPA. (solvent system: chloroform:acetone (1:1). C22:0 *sn*-2 MAG was the major product.

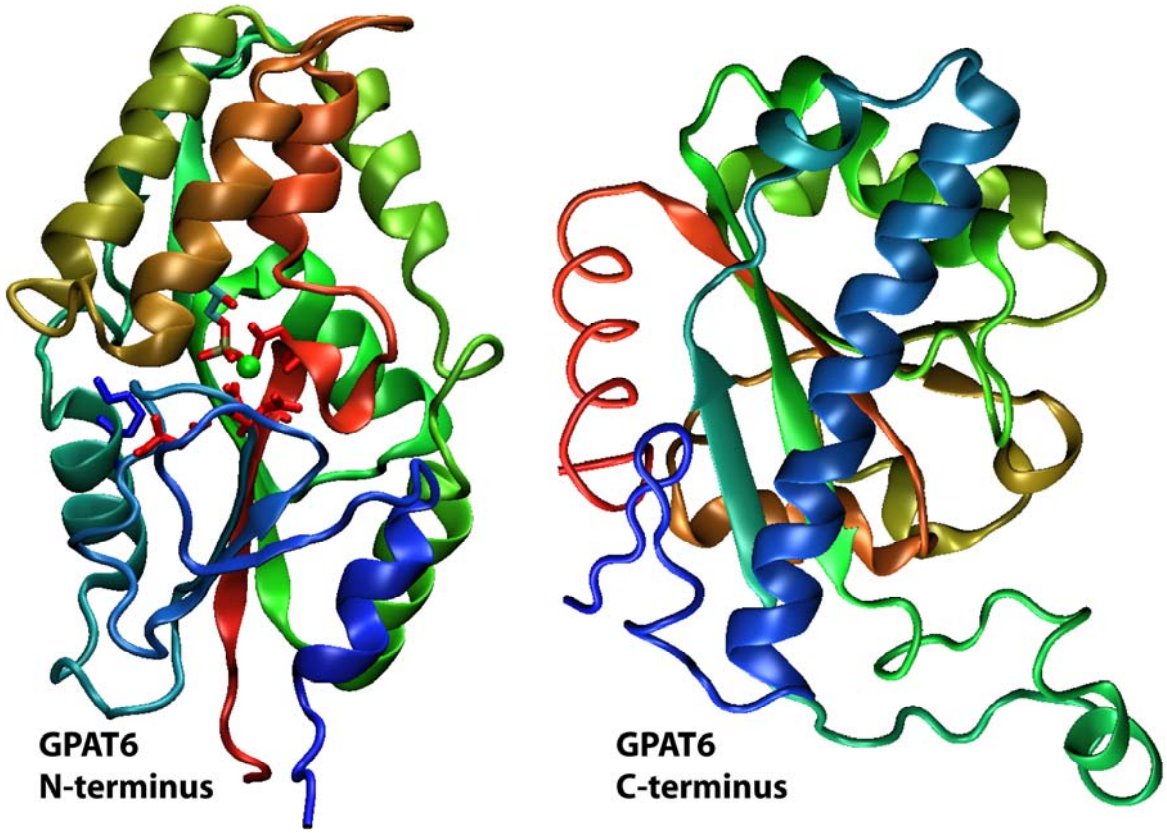

Fig. S8. **Complete Models for N- and C-terminal Domains of GPAT6 Based on *Methanococcus jannaschii* Phosphoserine Phosphatase (PDB: 1F5S) and Squash Glycerol-3-Phosphate (1)-Acyltransferase (PDB: 1K30), respectively.** Cartoon representation is colored by index (N-terminus (blue) to C-terminus (red)). Active site residues in N-terminal domain are shown as in Figure 5.

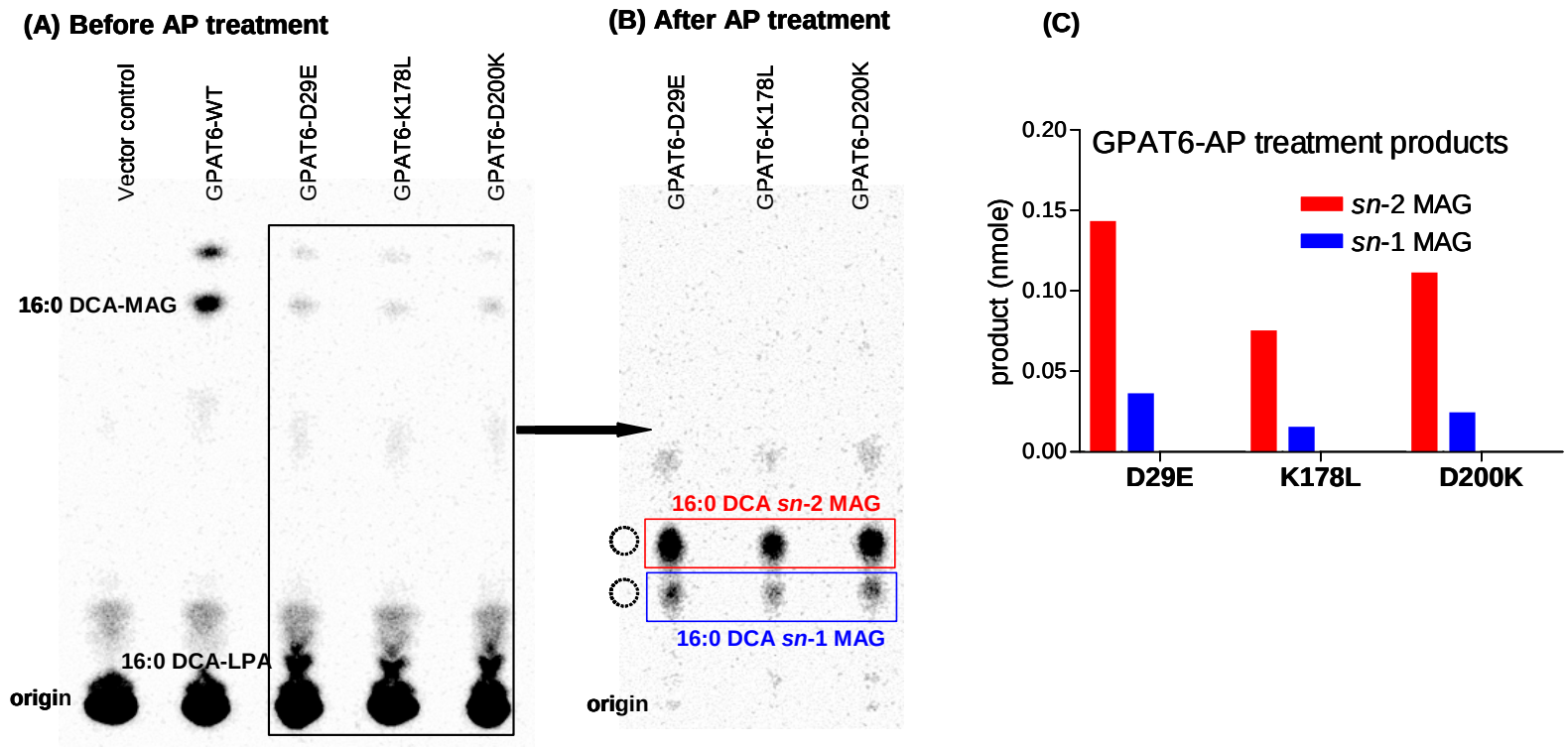

Fig. S9. Positional Analysis of C16:0 DCA-LPA from Assay of GPAT6 Site-Directed Mutants in Wheat Germ Cell-Free Translation System. GPAT assays were conducted using ^{14}C-G3P and C16:0 DCA-CoA as substrates. Two microliters of wheat germ translation reaction mixture of GPAT6 mutant (D29E, K178L or D200K) were used as the enzyme source, with GPAT6-WT and empty vector as the controls. (***A***) Radio-TLC image of product distribution of GPAT6 assay. C16:0 DCA-LPA was the major product for all three mutants. (***B,C***) Regiochemical analysis of LPA from assays of GPAT6 mutant forms. (***B***) Borate-TLC of products after immediate alkaline phosphatase (AP) treatment of the assay reaction. Products C16:0 DCA *sn*-1 and *sn*-2 MAGs were identified by co-migration with C18:1 DCA *sn*-1 and *sn*-2 MAG standards (dotted circles). (***C***) Product quantitation from borate-TLC analysis. In all three cases, *sn*-2 MAG is the predominant product derived from LPA hydrolysis.

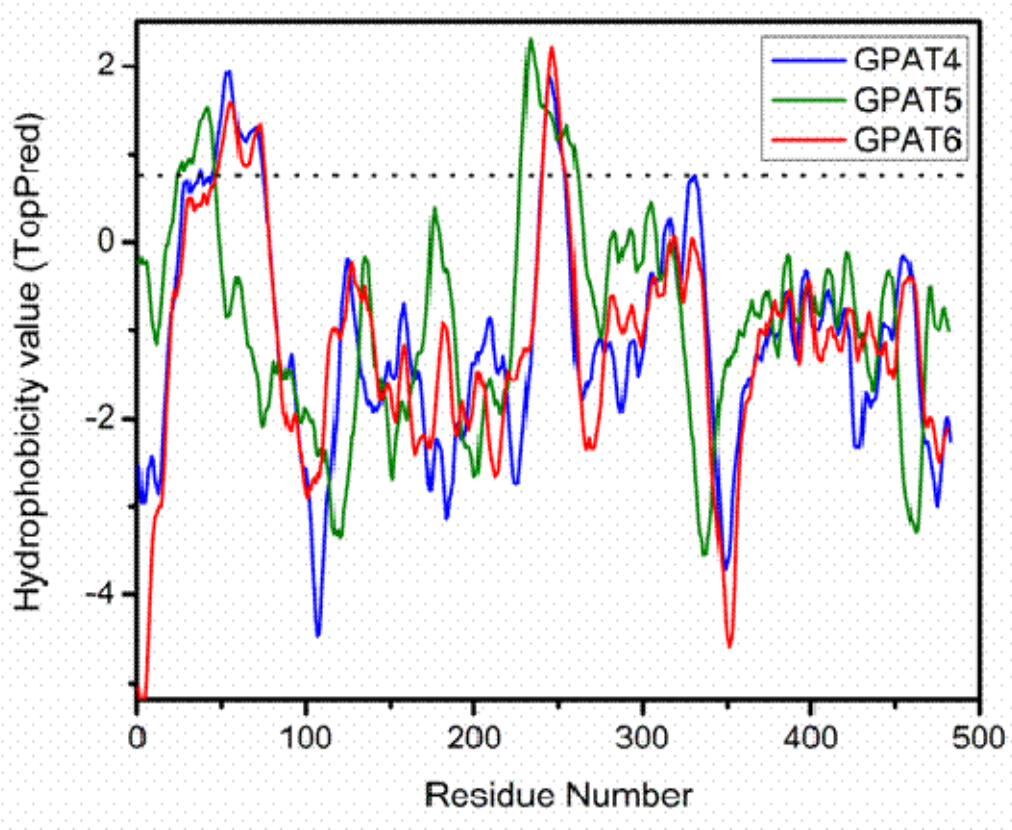

Fig. S10. Hydropathy plot for GPAT4, GPAT5, and GPAT6 sequences from TopPred (13) according to the Goldman-Engelman-Steitz hydrophobicity scale (14). The dotted line indicates an approximate cutoff above which transmembrane segments are likely. A transmembrane or membrane-associated region is predicted for residues 244-264 (GPAT4), 233-270 (GPAT5), and 246-266 (GPAT6). These residues separate the active/inactive phosphatase and acyltransferase domains of the proteins.

Motif I: DX**D**X[T/V][L/V]

```
Arab-GPAT4          --------MSPAKKSRSFPPISECKS---REYDSIAADLDGTLLLSRSSFPYFMLVAIEA
Arab-GPAT6          --------MGAQEKRRRFEQISKCDVK-DRSNHTVAADLDGTLLISRSAFPYYFLVALEA
XP_001769671        ------------MKRDPFDTIDKCSDK-GRSKQTVVSDLDGTLLRSRSSFPYFMLVAFEA
XP_001771186        ----MEVTKLKEAGNYSFAEVKSCSSGNDRRSQTVVADLDGTLIRGRSAFPYFFLVAFEA
XP_001753601        ---------MRKVRKYDFPIVGECSSGEHRKSETVIADLEGALMRARSSFPYFFLIAFEA
XP_001760362        ---MASLPEEFTHGEQRFQSLEKCS-TENRERQSIACDLYGTLVRSRASFPYFMLVAFEA
XP_001769724        METQEPDPVTSFHCSENYDEVENCRVE-GRANQSIVSDLDGTLLRSRSSFPYFMLLAFEA
XP_001765001        --MQQLDPLTSFHCSESFEGVETCRVE-GRANQSIVSDLDGTLLRSRSSFPYFMLLAFEA
XP_001780533        -MEIPGVFDANLFCAESFPEVETCKVE-GREKQTIISDLDGTLLRSRSSFPYFMLIAFDA
jgi_110301          ------MADLKYSRLFRFGLVENCSS-EGRGMHTVAADLDGTLLRGRSSFPYFLLVALEG
jgi_57.254.1        --------------MAEFPPIEKCSSTISRESESVASDLDGTLLRGRSSFPYFFLTTFET
```

Motif III: K-[G/S][**D**/S]XXX[**D**/N]

```
Arab-GPAT4          PGVLVGDLKRLAILKEFG---DDSPDLGLGDRTSDHDFMSICKEGYMVHETK-SATTVPI
Arab-GPAT6          PGILVGQYKRDVVLREFGGLASDLPDLGLGDSKTDHDFMSICKEGYMVPRTK-CEP-LPR
XP_001769671        PGVLTGRNKEIVLRQEFQG--LNLPDVGLGDRPSDHNFMSICKEGYIVPPSN-TILAASK
XP_001771186        PGVLVGTHKEEALKRCNIG--GERPHVGLGDRVTDFPFMAYCKEGYVVPKTK--VPAVKK
XP_001753601        PGVLVGAKKAEALKRWSMG--GERTHVGLGDQVTGYPFMAFCKEGYAVPRTK--VEAVRK
XP_001760362        PGVLLSMDKRNALKAACDG--KDAPDVGVGDRKHDHPFLTYCKEGYVVPADSGCQSAAPN
XP_001769724        PGVLVGTAKQRAVKKYFGS---DQPDLGLGDRTSDFAFMDLCKEAYIVPSYK-EVPSVTK
XP_001765001        PGVLVGAVKERAVKKYFGP---DPPDVGLGDRQSDFLFMDLCKESYIVHSDK-DVPAVSK
XP_001780533        AGVIVGANKTRAVKKYFGD---DLPDIALGDRASDFPFMALCKEAYLVPSFK-PVEPVAK
jgi_110301          PGVLVSQNKRTALKLEFVD--GELPEIGLGDRETDFAFMSLCKEAYVVPPSK--VEALSR
jgi_57.254.1        PGVLVGENKAKALLQACDP--EQLPDVGLGDRQTDFPFMKLCKEGYVVPPSN-NVEPVPK
```

Fig. S11. **Sequence Alignment of N-terminal Amino Acids of GPAT4 and GPAT6 with Primitive Moss, *Physcomitrella patens* (XP_n) and Spikemoss, *Selaginella moellendorffii* (jgi_n).** Partial sequences containing conserved motif I and III are shown. The conserved amino acid residues required for PSP activity in motif I and III are highlighted with colors.